

## **General Disclaimer**

### **One or more of the Following Statements may affect this Document**

- This document has been reproduced from the best copy furnished by the organizational source. It is being released in the interest of making available as much information as possible.
- This document may contain data, which exceeds the sheet parameters. It was furnished in this condition by the organizational source and is the best copy available.
- This document may contain tone-on-tone or color graphs, charts and/or pictures, which have been reproduced in black and white.
- This document is paginated as submitted by the original source.
- Portions of this document are not fully legible due to the historical nature of some of the material. However, it is the best reproduction available from the original submission.

X-624-77-123  
PREPRINT

*Tmx-71339*  
**MONTE-CARLO ANALYSIS OF  
UNCERTAINTY PROPAGATION IN A  
STRATOSPHERIC MODEL:  
II. UNCERTAINTIES DUE TO  
REACTION RATES**

(NASA-TM-X-71339) MONTE CARLO ANALYSIS OF  
UNCERTAINTY PROPAGATION IN A STRATOSPHERIC  
MODEL. 2: UNCERTAINTIES DUE TO REACTION  
RATES (NASA) 21 p HC A02/MF A01 CSCL 20N

N77-26349

Unclas  
G3/32 37030

**R. S. STOLARSKI  
D. M. BUTLER  
R. D. RUNDEL**

**MAY 1977**



**GODDARD SPACE FLIGHT CENTER  
GREENBELT, MARYLAND**

MONTE-CARLO ANALYSIS OF UNCERTAINTY PROPAGATION  
IN A STRATOSPHERIC MODEL:

II. UNCERTAINTIES DUE TO REACTION RATES

R. S. Stolarski and D. M. Butler  
NASA/Goddard Space Flight Center  
Laboratory for Planetary Atmospheres  
Greenbelt, Maryland 20771

R. D. Rundel  
NASA/Johnson Space Center  
Houston, Texas 77058

May 1977

GODDARD SPACE FLIGHT CENTER  
Greenbelt, Maryland

MONTE-CARLO ANALYSIS OF UNCERTAINTY PROPAGATION  
IN A STRATOSPHERIC MODEL:  
II. UNCERTAINTIES DUE TO REACTION RATES

R. S. Stolarski and D. M. Butler  
NASA/Goddard Space Flight Center  
Laboratory for Planetary Atmospheres  
Greenbelt, Maryland 20771

R. D. Rundel  
NASA/Johnson Space Center  
Houston, Texas 77058

ABSTRACT

A concise stratospheric model has been used in a Monte-Carlo analysis of the propagation of reaction rate uncertainties through the calculation of an ozone perturbation due to the addition of chlorine. Two thousand Monte-Carlo cases were run with 55 reaction rates being varied. Excellent convergence was obtained in the output distributions because the model is sensitive to the uncertainties in only about 10 reactions. For a 1ppbv chlorine perturbation added to a 1.5ppbv chlorine background, the resultant  $1\sigma$  uncertainty on the ozone perturbation is a factor of 1.69 on the high side and 1.80 on the low side. The corresponding  $2\sigma$  factors are 2.86 and 3.23. Results are also given for the uncertainties, due to reaction rates, in the ambient concentrations of stratospheric species.

# CONTENTS

	<u>Page</u>
A. INTRODUCTION . . . . .	1
B. CALCULATIONAL TECHNIQUE . . . . .	1
C. RESULTS . . . . .	3
D. DISCUSSION . . . . .	5
E. SUMMARY . . . . .	6
REFERENCES . . . . .	7

## TABLE

<u>Table</u>	<u>Page</u>
1 $1\sigma$ Uncertainty Limits on Column Ozone Depletion Due to a 1ppbv $Cl_x$ Perturbation for Different Numbers of Cases . . .	8

## ILLUSTRATIONS

<u>Figure</u>	<u>Page</u>
1     Logical flow diagram for Monte-Carlo stratospheric uncertainty propagation model . . . . .	9
2     Histogram of Monte-Carlo results for column ozone depletion above selected altitudes due to a 1ppbv $Cl_x$ perturbation . . . . .	10
3     Monte-Carlo results for ozone depletion above 15 km, plotted as $\log n$ versus $(\log r)^2$ to demonstrate the normality of the distribution . . . . .	11
4     Calculated one sigma uncertainty limits of $O_3$ and CO concentrations and of $CH_4$ and $N_2O$ mixing ratios . . . . .	12

# ILLUSTRATIONS (continued)

<u>Figure</u>		<u>Page</u>
5	Calculated one sigma uncertainty limits of NO, NO <sub>2</sub> and HNO <sub>3</sub> concentrations and of NO <sub>x</sub> mixing ratio . . . . .	13
6	Calculated one sigma uncertainty limits of O, OH, HO <sub>2</sub> and H <sub>2</sub> O <sub>2</sub> concentrations . . . . .	14
7	Calculated one sigma uncertainty limits of the ratios of Cl, ClO, HCl, and ClONO <sub>2</sub> to Cl <sub>x</sub> . . . . .	15
8	Calculated one sigma uncertainty limits of the ratios Cl/ClO, O/O <sub>3</sub> , and NO/NO <sub>2</sub> and of the O <sub>3</sub> column content . .	16

# MONTE-CARLO ANALYSIS OF UNCERTAINTY PROPAGATION IN A STRATOSPHERIC MODEL:

## II. UNCERTAINTIES DUE TO REACTION RATES

### A. INTRODUCTION

Rundel et al. (1977), hereafter referred to as Paper I, have described the derivation of a concise stratospheric model designed to be used in a Monte-Carlo analysis of uncertainty propagation. One of the greatest difficulties in carrying out such an analysis is the proper characterization of the uncertainty distribution of the input parameters. A one-dimensional model of the stratosphere has many input parameters; reaction rates, cross sections, solar intensity, transport parameters, temperature distribution,  $N_2$  and  $O_2$  model atmosphere. The most important sources of uncertainty in ozone depletion calculations, as identified by the National Research Council Panel on Atmospheric Chemistry (1976) are the reaction rates and transport parameters. Transport is usually represented in a one-dimensional model as a diffusion coefficient. This diffusion coefficient is meant to approximate the average effect of the mean global circulation system and departures from this mean. This approximation is not well enough understood to allow one to quantify its uncertainty. However, the reaction rates included in current stratospheric chemistry models have been the subject of many laboratory studies over the past few years and, with a few notable exceptions, are rapidly becoming well enough known to make a reasonable estimate of their uncertainty possible. This paper demonstrates the application of the concise model described in Paper I to the propagation of reaction rate uncertainties through typical stratospheric model calculations.

### B. CALCULATIONAL TECHNIQUE

Uncertainties in rate constants used in stratospheric models range from rather small (approximately a factor of 1.1) to very large (up to a factor of 10). Since all reaction rates must be positive, the appropriate probability distribution to assume is the log normal distribution (Aitchison and Brown, 1969). The probability that the true reaction rate lies between  $k$  and  $k+\Delta k$  is given by

$$p(k) = (\sqrt{2\pi} \sigma k)^{-1} \exp \left[ -\frac{1}{2\sigma^2} (\log k - \log k_0)^2 \right] dk$$

where  $\log k_0$ , the logarithm of the actual measured value, is the mean value of  $\log k$ ; and  $\sigma$ , the logarithm of the estimated uncertainty factor, is the standard deviation of  $\log k$ . The use of this distribution is equivalent to assuming that  $\log k$  is normally distributed. This is a physically reasonable distribution in that laboratory experiments typically measure  $\log k_0$  rather than  $k_0$  itself (R. Watson, personal communication).

Figure 1 is a logical flow diagram showing how these probability distributions are used in the concise stratosphere model to determine the uncertainty propagation properties of that model. First, the model is run to steady-state (<1 part in 5000 change in ozone concentration at any altitude per iteration step) with the chosen "best set" of reaction rates. This steady-state ambient result includes 1.5 ppbv C1X resulting from 1 ppbv methyl chloride, ( $\text{CH}_3\text{Cl}$ ) and 0.1 ppbv carbon tetrachloride, ( $\text{CCl}_4$ ) at the lower boundary added to a 0.1 ppbv C1X lower boundary condition. A chlorine perturbation of the desired magnitude is then added, the model is run to steady-state, and the change in column ozone, alone with other parameters, is determined. A random number generator is then used to generate a set of random numbers  $\epsilon_i$ , with zero mean and unity standard deviation. New values for rates  $k_i$  are then determined from

$$\epsilon_i = (\log k_i - \log k_{oi})/\sigma_i$$

When all 55 rates have been thus perturbed the model is again run to steady-state with 1.5 ppbv C1X. The desired chlorine perturbation is then added to this model, it is run to the new steady-state, and the resulting ozone column depletion is recorded. The values of all the species concentrations before addition of the perturbation are also recorded. This process is then repeated by choosing another set of 55 random numbers, applying each to a reaction, and re-running the model with and without the perturbation. When 200 cases are accumulated the resulting distributions for the logarithms of ozone column depletion, ozone column density, species densities and ratios of species densities, are fitted to separate normal distributions on the high and low side of the mean values. (This procedure recognizes the fact that, due to non-linear feedback mechanisms, uncertainty distributions of model outputs may be skewed.) Further groups of 200 are then run until the accumulated one sigma uncertainties on both sides of the distribution have converged to within one or two percent. In all 2000 cases were run although satisfactory convergence for column ozone depletion was obtained after 1200 cases. For most of the species concentrations the convergence was significantly more rapid although for a few of the species in the methane oxidation chain, where reaction rates are very uncertain, only poor convergence was achieved. Table 1 shows an example of the cumulative 1 $\sigma$  uncertainty bound for column ozone depletion at intervals of 200 cases. Obviously the mean would have been approached in a different manner had the cases been taken in a different order. Also shown are the 1 $\sigma$  uncertainties for each of the groups of 200 cases independent of all of the other groups. (Note that the average  $\sigma$  for the ten 200 case groups is greater than the  $\sigma$  for all 2000 cases. This is because each 200 case group must be weighted according to how well it approximates normality, and this weighting factor tends to be smaller for groups with larger values of  $\sigma$ .)



## C. RESULTS

Figure 2 is a histogram of the 2000 cases of column ozone depletion above 4 different altitudes, 45 km, 35 km, 25 km, and 15 km, which is the lower boundary of the model. All of these results are for a perturbation of 1 ppbv  $C1_x$  in the asymptotic limit added to a 1.5 ppbv background due to  $CH_3Cl$  and  $CCl_4$  as described above. The horizontal axis represents the ratio  $r$  of the fractional change in ozone column with randomly chosen rates to the value obtained with the "best set" of rates, plotted on a logarithmic scale. The bin size is chosen such that  $\Delta(\log r)$  is constant. The histograms for ozone depletion above 35 and 45 km show a slight negative skewness, which is most likely an example of a saturation effect. In general, a saturation effect can be expected to occur when the ozone destruction efficiency is high because most of the chlorine is in the form  $C1$  or  $C10$  and hence is participating directly in catalytic destruction. As can be seen from the figure, the slight skewness at high altitudes is essentially gone in the column above 15 km indicating that, within the range of depletions represented, the catalytic efficiency is not near the saturation value. Figure 2 also shows distribution widths which are larger at 15 and 45 km than at the middle altitudes. The larger width at 45 km is a result of control by  $HO_x$  catalytic reactions which are more uncertain than those of  $O_x$ ,  $NO_x$ , or  $C1_x$ . This effect is gradually washed out as the column is extended downward. The increase in distribution width in the total column above 15 km is due to the uncertainty inherent in the subtraction of the low altitude self-healing effect from the high altitude destruction and to reactions involving  $HO_x$ .

Figure 3 shows a plot, for the case of ozone depletion above 15 km, of the logarithm of the number of cases in each bin as a function of  $(\log r)^2$  for each side of the distribution. In these coordinates a normal distribution with zero mean should give a straight line of slope  $1/\sigma$ . The best weighted straight line fit is shown. The resulting uncertainties in column ozone depletion are shown in Table 1. For a 1 ppbv  $C1_x$  perturbation, the  $1\sigma$  uncertainty due to reaction rates alone is a factor of 1.69 on the high side and a factor of 1.80 on the low side. The corresponding  $2\sigma$  uncertainties factors are 2.86 and 3.23. For the case of continuing release of fluorocarbons 11 and 12 at their 1975 rates until steady-state is reached (resulting in a 5.7 ppbv  $C1_x$  perturbation)  $1\sigma$  uncertainty factors of 1.7 and 1.8 on the high and low sides, respectively, were obtained. These correspond to  $2\sigma$  factors of 2.8 and 3.1 and are based upon an aggregate of only 800 cases.

Figures 4-8 show a series of altitude profiles of stratospheric concentrations and ratios of concentrations. For each profile a range is shown corresponding to the  $1\sigma$  confidence limits calculated from the unperturbed atmosphere (which has 1.5 ppbv  $C1_x$ ).

Figure 4 shows the  $1\sigma$  uncertainties in  $O_3$  and CO concentration and in  $CH_4$  and  $N_2O$  mixing ratio. These latter are calculated in the model by solving a diffusion equation with a fixed lower boundary condition; thus, any uncertainty at 15 km has been suppressed. The uncertainty increases with increasing distance from the boundary because at higher altitudes the mixing ratio is determined in large part by what has happened below and this leads to a build up in uncertainty. For total odd nitrogen, another diffused quantity shown in Figure 5, the lower boundary condition is unimportant compared with the stratospheric source and the uncertainty in mixing ratio is roughly constant above 15 km. The uncertainties in NO above 45 km and in  $HNO_3$  at 15 km are constrained by the uncertainty in total odd nitrogen, since at those altitudes these species dominate this group.

Uncertainties in solar flux and photolysis cross sections (which are not included in the present model) have been found to make only small contributions to the overall uncertainty in chlorine induced ozone perturbations (NRC Panel, 1976). However, this does not insure that these uncertainties will be unimportant for other model results. Care must be taken to correctly interpret the uncertainty limits calculated for any quantity for which reaction rate uncertainty is small and photolysis is important. Examples of this are included in the discussion below.

The uncertainties in O,  $O_3$ ,  $O_3$  column, and the O/ $O_3$  ratio merit detailed examination. Ozone itself comprises virtually all of odd oxygen in the altitude range considered, and except at 15 km, odd oxygen is essentially produced solely by  $O_2$  photolysis (see Figure 2 of paper I). Therefore, in the present model the uncertainty in odd oxygen above 15 km is entirely due to the uncertainty in destruction reactions. Over much of the stratosphere the principal destruction reaction is  $NO_2 + O \rightarrow NO + O_2$ , for which the rate is believed to be exceptionally well known. At the upper and lower boundaries, reactions of greater uncertainty are important and the resulting  $O_3$  uncertainty is found to be greater at these altitudes (see Figure 4). The O/ $O_3$  ratio only depends upon the photolysis of ozone and its formation reaction  $O + O_2 + M \rightarrow O_3 + M$  for which the uncertainty in the rate is small. Thus, the uncertainty of this ratio is small, and taken together with the small uncertainty in  $O_3$ , this yields a small uncertainty in O (see Figure 6).

Figure 7 shows the uncertainties in relative amounts of the four  $Cl_x$  species. In practice, the uncertainties were calculated for the species concentrations individually, but the total  $Cl_x$  mixing ratio at any height is subject to only negligible errors. This is because of (1) fixed lower boundary conditions on  $Cl_x$  and its source molecules, (2) the exclusion of cross section and solar flux uncertainties in the present model, and (3) the small uncertainty in  $O_3$  column density. The last of these is in fact the only source of uncertainty present in the model

which affects total  $C1_x$ . This constraint on total  $C1_x$  explains the small uncertainty in HC1 at high and low altitudes where virtually all  $C1_x$  is HC1.

The  $C1/C10$  ratio (see Figure 8) is dependent upon the concentrations of O, NO and  $O_3$  and upon three reaction rates ( $C1 + O_3 \rightarrow C10 + O_2$ ,  $C10 + O \rightarrow C1 + O_2$ ,  $C10 + NO \rightarrow C1 + NO_2$ ). The relatively larger uncertainty in the NO reaction rate together with the range of NO concentration shown in Figure 5 are the principal cause of the large uncertainty in this ratio except at high altitudes where the O channel becomes the dominant path for C10 reaction and here the uncertainty narrows considerably.

#### D. DISCUSSION

The Monte-Carlo technique has a promising application to the analysis of atmospheric concentration measurements. Specifically, when the ratio of concentrations of two constituents is measured, and the chemical time constants connecting these species are short compared to transport times, a one dimensional model can be expected to predict the ratio. Specific examples are  $O/O_3$ ,  $C1/C10$ , and  $NO/NO_2$ . Figure 8 shows calculated profiles for these ratios indicating the 1 $\sigma$  confidence limits. Some care, however, must be exercised in directly using these results in model-measurement comparisons. The ratios, while chemically controlled, are sensitive to meteorological variability. The  $O/O_3$  ratio depends on a dissociation coefficient and hence on the column of ozone above the measurement.  $C1/C10$  depends  $O/O_3$  at high altitude and on O, NO, and  $O_3$  at lower altitude.  $NO/NO_2$  depends on local  $O_3$ . Thus, a well-designed experiment should measure not only one of these ratios but the concentrations of the species controlling it. Then a Monte-Carlo analysis on a restricted model which fixes the meteorologically varying components at measured values will yield calculational uncertainties from which an assessment of agreement or disagreement between measurement and theory can be made.

The information content in such comparisons depends on the relative uncertainty bounds which can be placed on the theoretical calculation and on the measurement. When the experimental uncertainties are much larger than the theoretical ones the information content on how well the experiment confirms the theory is directly proportional to the experimental uncertainty. When the two uncertainty bounds are comparable maximum confirmation information is obtained. When the experimental uncertainties are significantly smaller than the theoretical uncertainties the possibility exists for obtaining rate information. However, firm conclusions from this type of information should be avoided because of the possibility that some reaction of significance has not been included in the model.

## E. SUMMARY

This study demonstrates the effect of reaction rate uncertainty on the results of a one dimensional stratospheric chemistry model. Since the model results are particularly sensitive to only about 10 of the more than 50 reaction rates included only about  $2^{10}$  or  $\sim 1000$  Monte-Carlo cases are needed to reasonably span the space of possible results. This contrasts with the more than  $2^{50}$  calculations claimed necessary by Stewart and Hoffert (1975). This would be the case only if the model were approximately equally sensitive to all of the reactions included.

The uncertainties on column ozone depletion are larger than those determined by the NRC panel. Their report gives a  $2\sigma$  uncertainty on ozone depletion due to reaction rates of 2.4 deduced from a sensitivity study of 7 key reactions. The Monte-Carlo technique yields approximately a factor of 3 for the  $2\sigma$  uncertainty due to the variation of 55 rate constants. The somewhat larger number obtained is not particularly surprising in view of the added reactions considered.

This calculation provides a means of assessing the uncertainty in model results caused by model inputs in a comprehensive manner which includes all the interactions of input parameter uncertainties. The feasibility of using this technique will always rest upon the computer time required to run the underlying model and upon the number of cases required to obtain convergence in the distributions of output values. Within this constraint, the calculation can be extended by improving the basic model and by including uncertainties in solar flux, photolysis cross sections, assumed mixing ratios of constituents, temperature and other inputs besides reaction rates. The results will need to be redetermined if and when there are substantial changes in the rate constants or their uncertainties or in the basic understanding of stratospheric processes.

## REFERENCES

Aitchison, J. and J. A. C. Brown, The Lognormal Distribution, Cambridge University Press, 1969.

National Research Council Panel on Atmospheric Chemistry, Halocarbons: Effects on Stratospheric Ozone, Washington, D.C., September 1976.

Rundel, R. D., D. M. Butler, and R. S. Stolarzki, Monte-Carlo Analysis of Uncertainty Propagation in a Stratospheric Model: I. Development of a Concise Stratospheric Model, submitted to J. Geophys. Res., 1977.

Stewart, R. W. and M. I. Hoffert, Stratospheric Ozone - Fragile Shield, Astronautics and Aeronautics, 13, 42, October 1975.

**Table 1**

**1 $\sigma$  Uncertainty Limits on Column Ozone Depletion Due to a  
1ppbv Cl<sub>x</sub> Perturbation for Different Numbers of Cases**

<b>Number of Cases</b>	<b>Low Side Uncertainty</b>	<b>High Side Uncertainty</b>
200	2.16	1.83
200	1.96	1.72
200	1.74	1.90
200	2.20	1.70
200	1.71	1.75
200	1.96	1.70
200	1.83	1.85
200	2.08	1.78
200	2.19	1.75
200	1.72	1.67
400	1.92	1.75
600	1.86	1.77
800	1.84	1.71
1000	1.80	1.69
1200	1.80	1.69
1400	1.79	1.71
1600	1.80	1.71
1800	1.81	1.71
2000	1.80	1.69

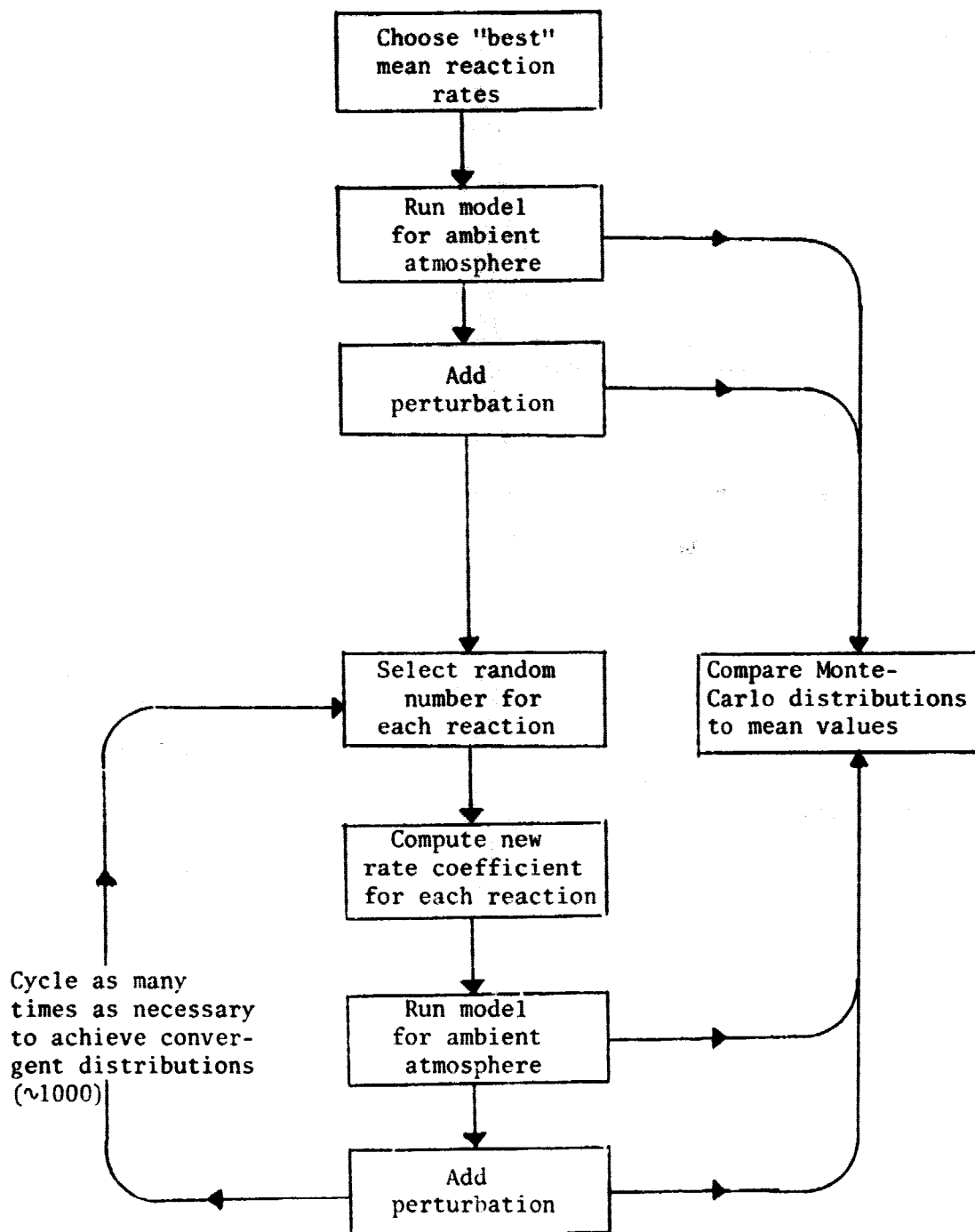
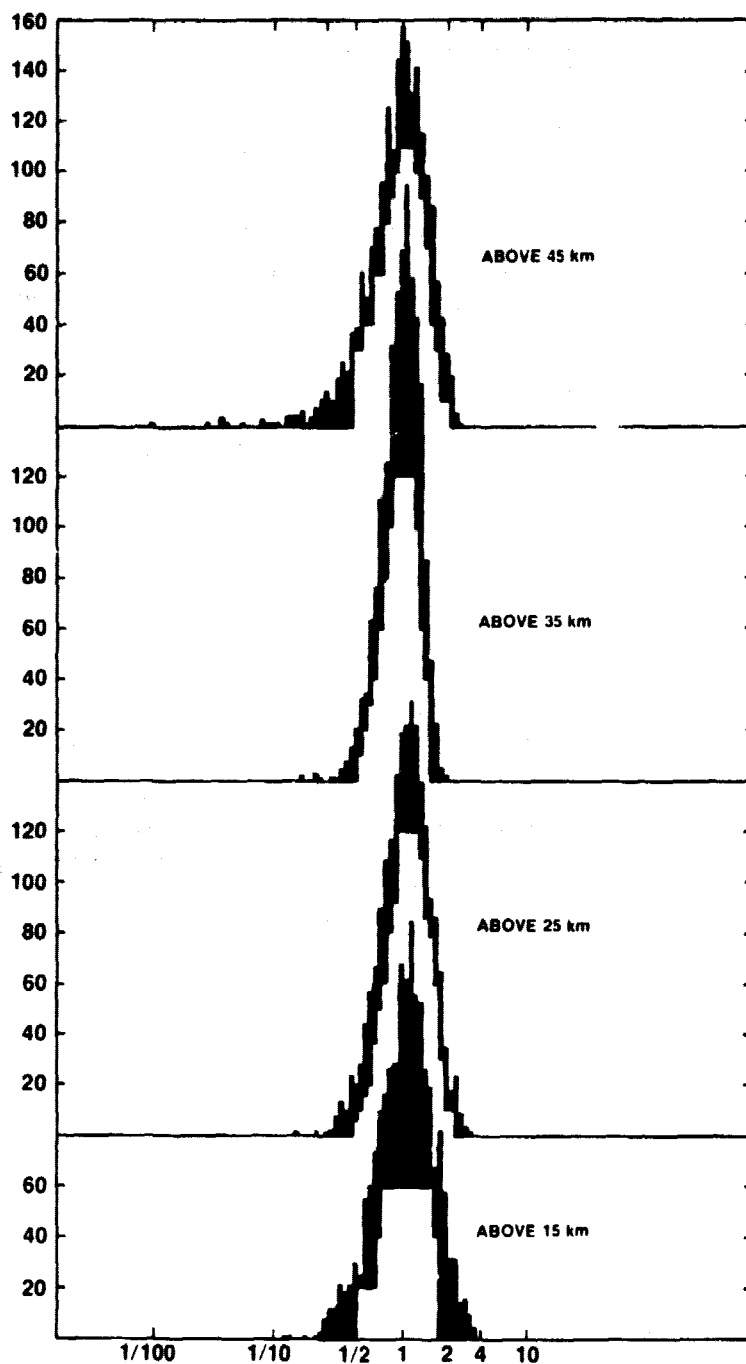


Figure 1. Logical flow diagram for Monte-Carlo stratospheric uncertainty propagation model.



DISTRIBUTION OF OZONE COLUMN DEPLETION ABOVE A HEIGHT

Figure 2. Histogram of Monte-Carlo results for column ozone depletion above selected altitudes due to a 1 ppbv  $\text{Cl}_x$  perturbation (see text).



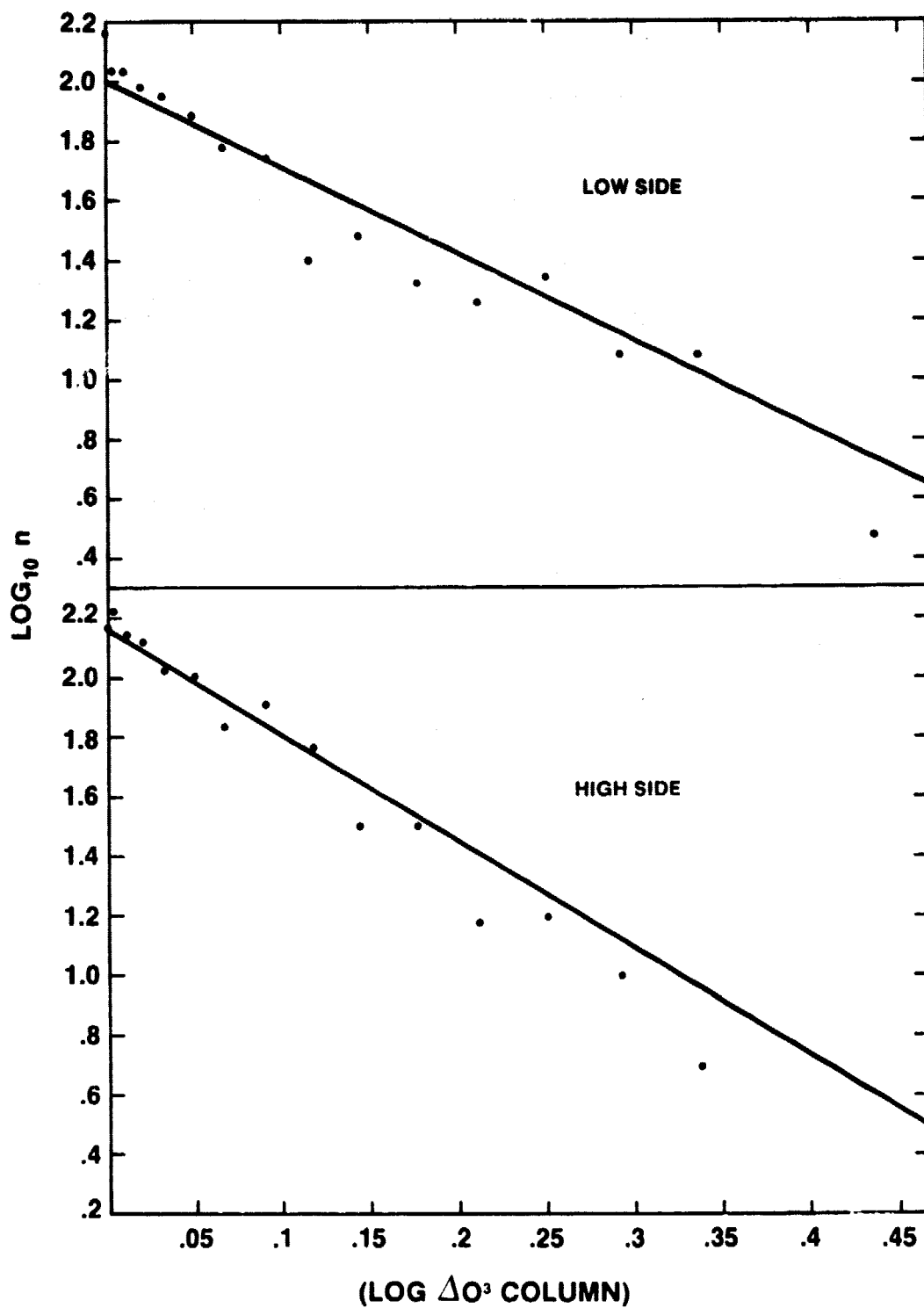


Figure 3. Monte-Carlo results for ozone depletion above 15km, plotted as  $\log n$  versus  $(\log r)^2$  to demonstrate the normality of the distribution (see text).

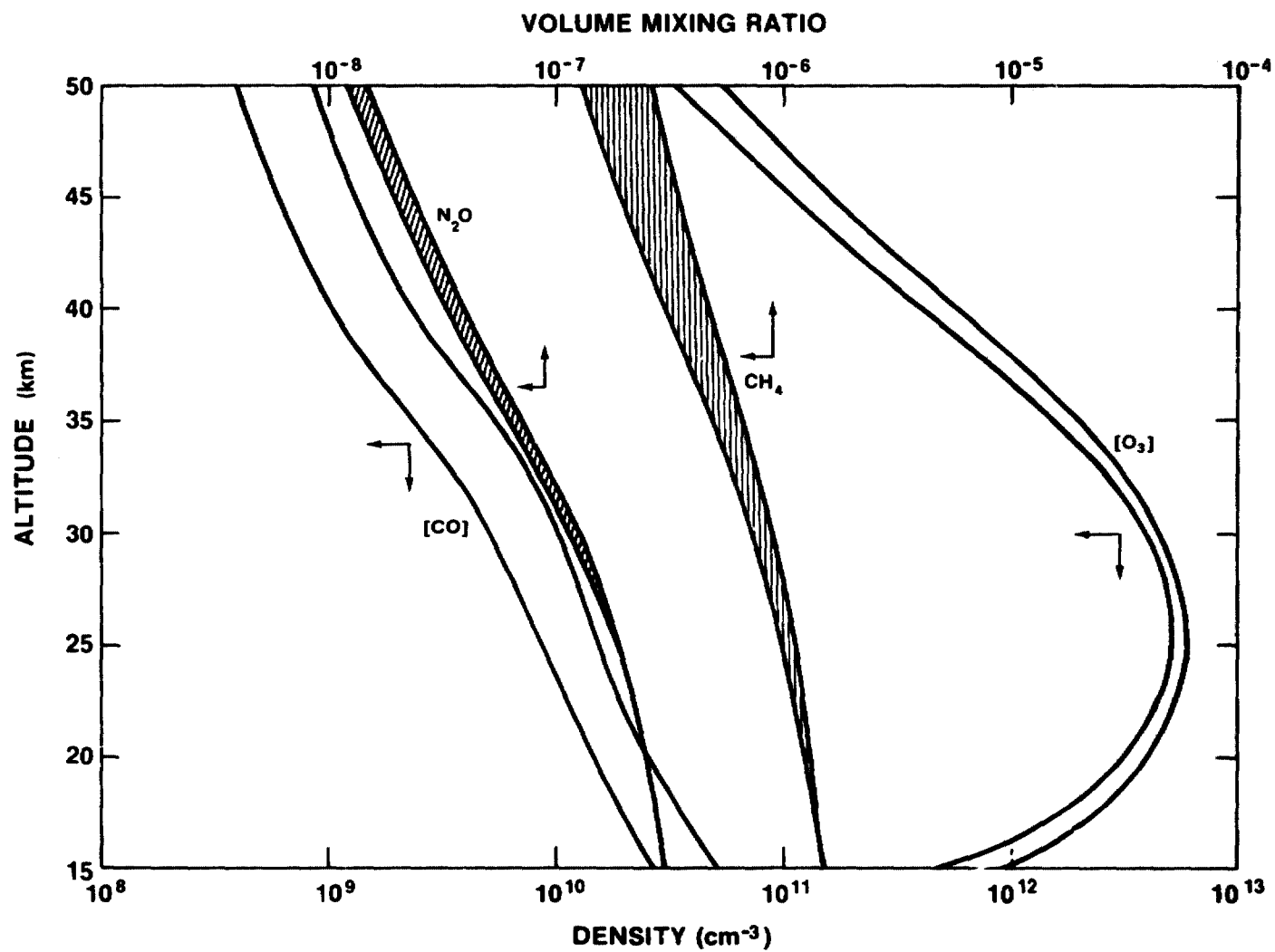


Figure 4. Calculated one sigma uncertainty limits of  $\text{O}_3$  and CO concentrations and of  $\text{CH}_4$  and  $\text{N}_2\text{O}$  mixing ratios.

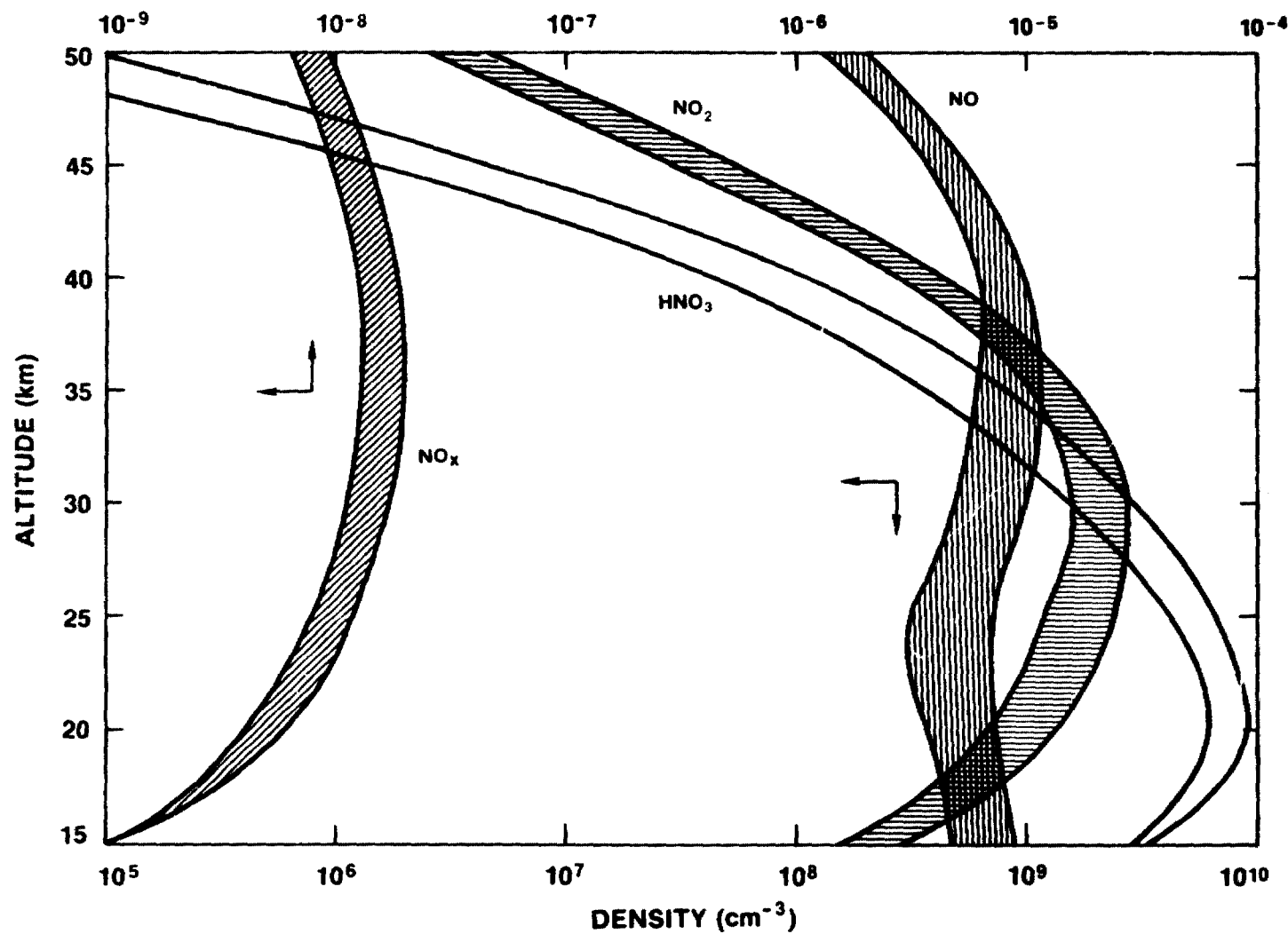


Figure 5. Calculated one sigma uncertainty limits of NO,  $\text{NO}_2$  and  $\text{HNO}_3$  concentrations and of  $\text{NO}_x$  mixing ratio.

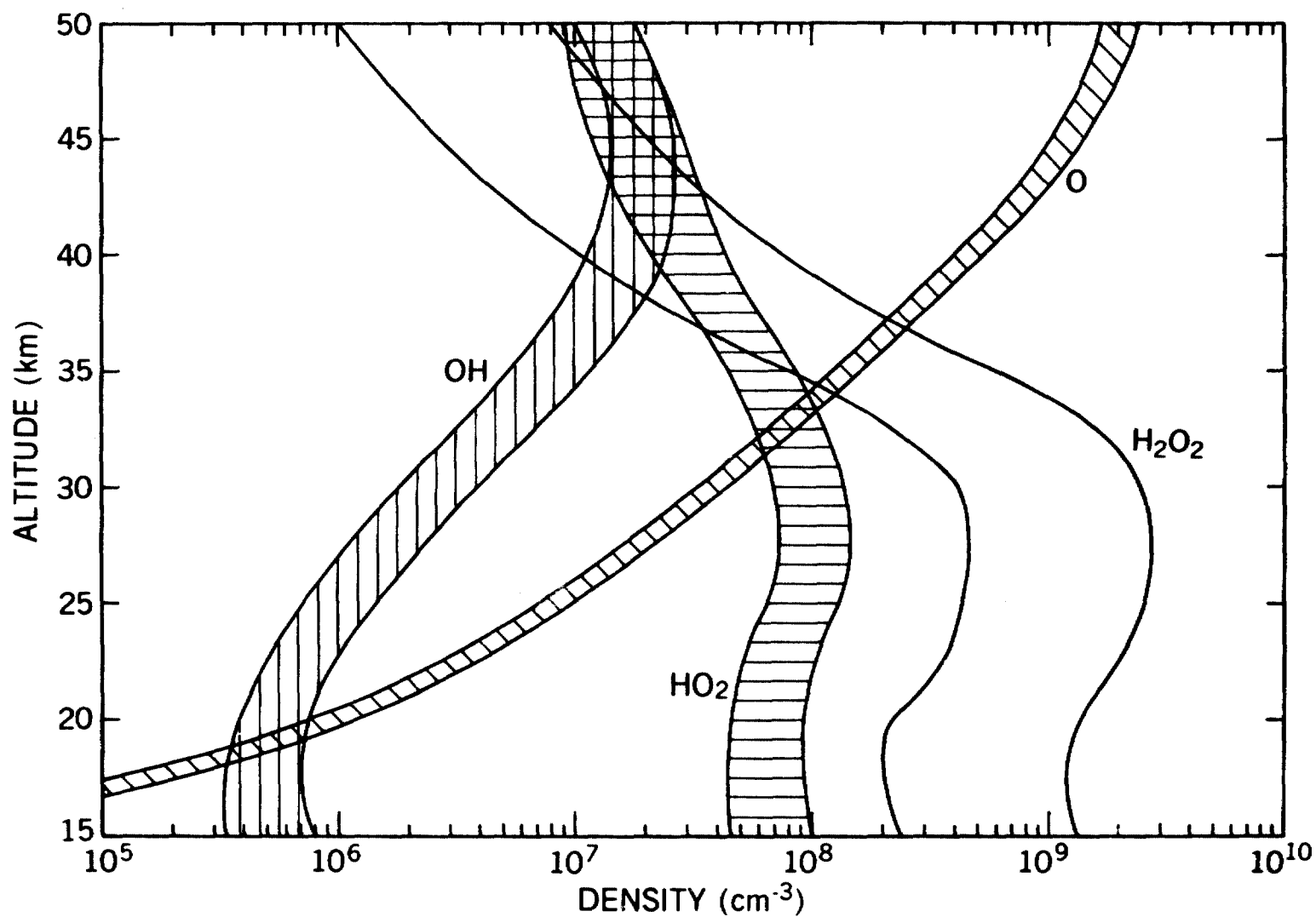


Figure 6. Calculated one sigma uncertainty limits of O, OH, HO<sub>2</sub> and H<sub>2</sub>O<sub>2</sub> concentrations.

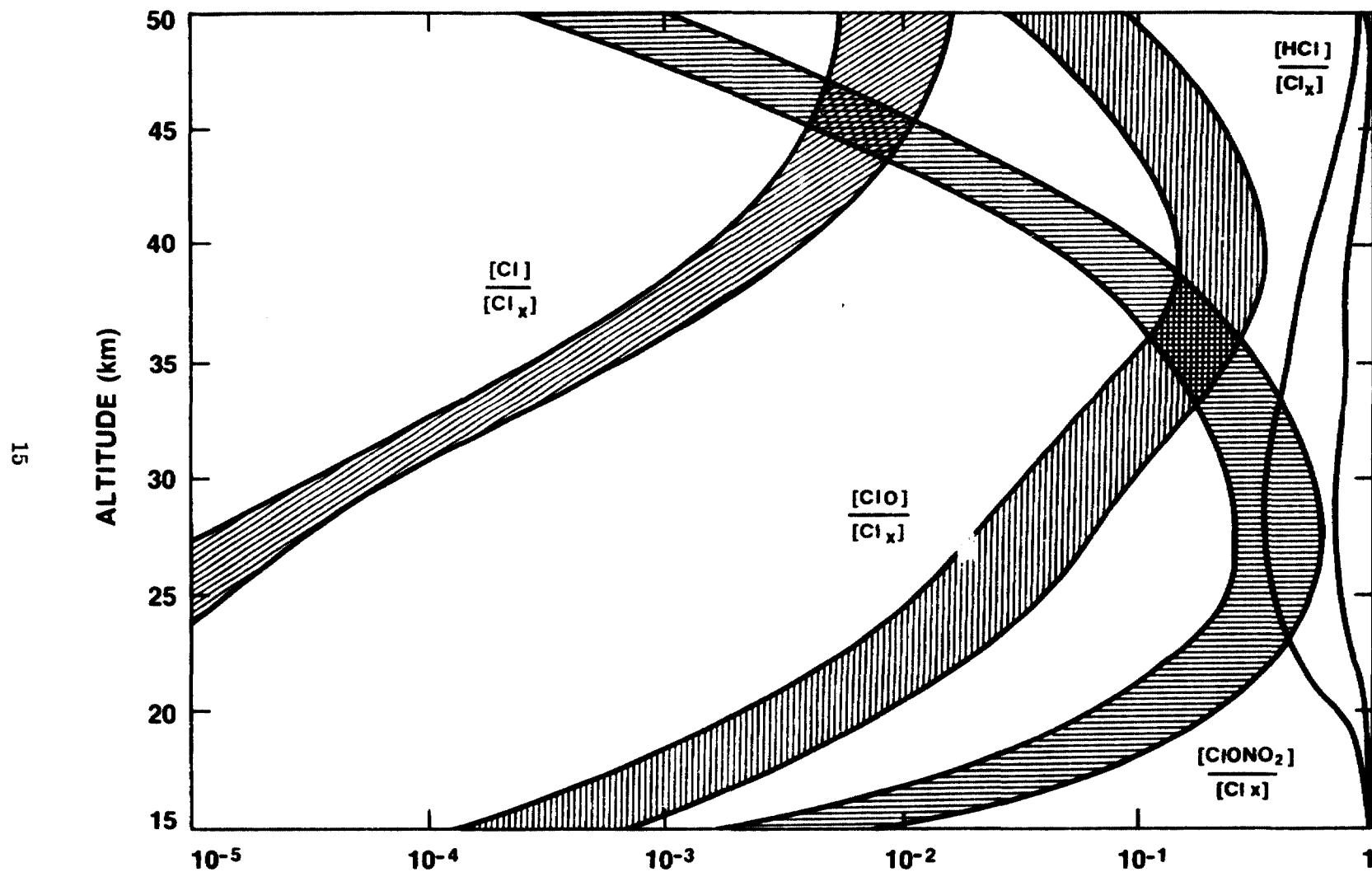


Figure 7. Calculated one sigma uncertainty limits of the ratios of Cl, ClO, HCl, and ClONO<sub>2</sub> to Cl<sub>x</sub>.

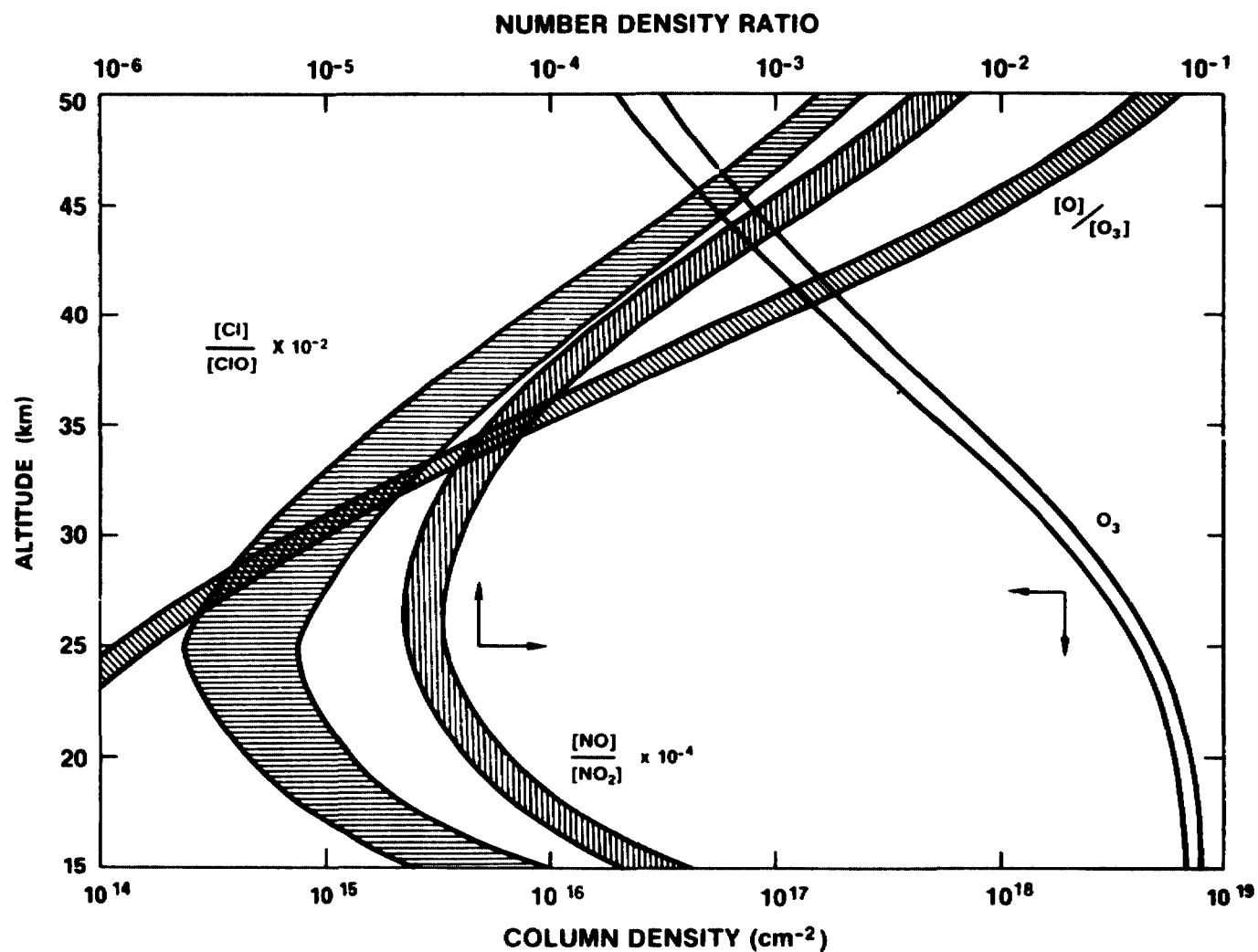


Figure 8. Calculated one sigma uncertainty limits of the ratios  $\text{Cl}/\text{ClO}$ ,  $\text{O}/\text{O}_3$ , and  $\text{NO}/\text{NO}_2$  and of the  $\text{O}_3$  column content.